Overcoming Challenges of MEG/EEG Data Analysis: Insights from Biophysics, Anatomy, and Physiology

Matti S. Hämäläinen, PhD

Athinoula A. Martinos Center for Biomedical Imaging
Massachusetts General Hospital
Charlestown, Massachusetts

Introduction

By noninvasively measuring electromagnetic signals ensuing from neurons, magnetoencephalography (MEG) and electroencephalography (EEG) are the only noninvasive human brain imaging tools that provide submillisecond temporal accuracy. In this way, they help to unravel precise dynamics of brain function. Functional magnetic resonance imaging (fMRI) provides a spatial resolution in the millimeter scale, but its temporal resolution is limited because it measures neuronal activity indirectly by imaging the sluggish hemodynamic response. In contrast, MEG and EEG measure the magnetic and electric fields that are directly related to the underlying electrophysiological processes and can thus attain their high temporal resolution.

Processing MEG or EEG data to obtain accurate localization of active neural sources is a complicated task. It involves numerous steps: signal denoising; segmenting various structures from anatomical MRIs; numerical solution of the electromagnetic forward problem; a solution to the ill-posed electromagnetic inverse problem; and appropriate control of multiple statistical comparisons spanning space, time, and frequency across experimental conditions and groups of subjects. This complexity not only constitutes a challenge to MEG investigators but also offers a great deal of flexibility in data analysis.

However, thanks to the direct relationship between the MEG and EEG signals and the underlying neural currents, much insight into these methods can be gained by understanding the associated biophysics in the context of neurophysiology and anatomy. This chapter discusses the relationship of the macroscopic MEG and EEG signals and their physiological sources, thus providing the foundation for understanding the analysis methods applied to estimate the time courses of brain activity. It also gives an overview of available source estimation methods to help beginners understand their underlying assumptions and their applicability to particular experimental data.

Sources and Fields

Neuronal currents generate magnetic and electric fields according to Maxwell's equations. This current distribution can be described as the primary current, the "battery" if you will, in a resistive circuit that comprises the head. The postsynaptic currents in the cortical pyramidal cells are the main primary currents giving rise to measurable MEG/EEG signals. In many calculations, the head can be approximated with a spherically symmetric conductor; however, more realistic head models for field calculations can be constructed with the help of anatomical magnetic resonance (MR) or computed tomography (CT) images.

If we employ the spherically symmetric conductor model, the magnetic field of a current dipole can be derived from a simple analytic expression (Sarvas, 1987). An important feature of this sphere model is that the result is independent of the conductivities and thicknesses of the spherical layers; it is sufficient to know the center of symmetry. In contrast, calculating the electric potential is more complicated and requires full information on conductivity. Because radial currents do not produce any magnetic field outside a spherically symmetric conductor, MEG to a great extent is selectively sensitive to tangential sources. EEG data are thus required for recovering all components of the current distribution. Since the resultant current orientation on the cortex is normal to the cortical mantle, MEG is selectively sensitive to fissural activity (Fig. 1).

The analytic sphere model provides accurate enough estimates for many practical purposes. However, when the source areas are located deep within the brain or in frontal areas, it is necessary to use more accurate approaches (Mosher et al., 1999). Within a realistic geometry of the head, the Maxwell's equations cannot be solved without resorting to numerical techniques. In the boundary-element method (BEM), the electrical conductivity of the head is assumed to be piecewise homogeneous and isotropic. Under these conditions, electric potential and magnetic field can be calculated numerically, starting from integral equations that are discretized to linear matrix equations (Hämäläinen and Sarvas, 1989; Mosher et al., 1999).

The conductivity of the skull is low; therefore, most of the current associated with brain activity is limited to the intracranial space. A highly accurate model for MEG is obtained by considering only one homogeneous compartment bounded by the skull's inner surface (Hämäläinen and Sarvas, 1989). The boundary-element model for EEG is more complex because at least three compartments need to be considered: the scalp, the skull, and the brain.

It is also possible to employ the finite-element method (FEM) or the finite difference method (FDM) for solving the forward problem. The solution is then based directly on the discretization of the Poisson equation governing the electric potential. In this case, any three-dimensional conductivity distribution and even anisotropic conductivity can be incorporated.

NOTES

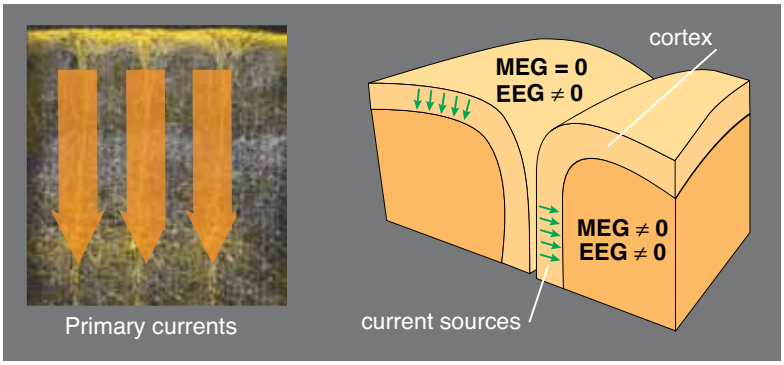

Figure 1. Principal orientation of primary currents on the cortex (left). Differential sensitivity of MEG and EEG in the presence of cortical folding (right).

Thanks to improvements to computational methods, FEM approaches are being introduced into routine use in source modeling algorithms that require repeated calculation of the magnetic field from different source distributions (Wolters et al., 2004).

As discussed above, MEG signals can be computed to a high level of accuracy without referring to the particular electrical conductivity values within the head. Therefore, MEG is likely to provide more accurate estimates of the current strengths than EEG. Combined with information about the feasible current densities on the cortex (Okada et al., 1997; Murakami et al., 2002), it is thus possible to infer the sizes of the activated cortical areas. These current density estimates are in the range of 0.1–1.0 nAm/mm^2, translating a typical 20 nAm current dipole observed in MEG/EEG to a cortical area of 20–200 mm^2.

Sensitivity Characteristics of MEG and EEG

In general, electric and magnetic fields decay as a function of distance from the underlying sources. However, other important factors affect the sensitivity of MEG and EEG to activity in different brain structures. These factors include the organization of the active cell assemblies, effects of the almost spherical symmetry of the head, macroscopic spatial cancellation effects, and extent of temporal coherence of the source activity.

As shown in Figure 1, the cortex has a cellular organization favoring the generation of strong MEG and EEG signals: The pyramidal cells are oriented in parallel and normal to the cortical mantle, making it possible for the electromagnetic fields from postsynaptic currents in individual cells to add up constructively to produce measurable fields. Such inference is much more difficult to make for small deeper structures, even though it has been clearly shown that both EEG and MEG signals can be produced, for example, by the brainstem nuclei (Parkkonen et al., 2009). Using simulations, it also has been shown that, in the absence of simultaneous cortical activity, hippocampal activity can be detected with standard source localization methods (Attal and Schwartz, 2013). The same study also found that it is possible to detect weak thalamic modulations of ongoing activity. Furthermore, MEG has provided insights into the specific dissociated neural pathways involved in emotion and face perception, including sources in both the cortex and the amygdalae (Hung et al., 2010).

It is important to note that since the spherically symmetrical conductor model well approximates the computation of MEG/EEG, the overall conclusion regarding the relative sensitivities of the two methods remains valid even in a more realistic head model. Figure 2 illustrates the distribution of MEG and EEG sensitivity across the cortex when the signals are

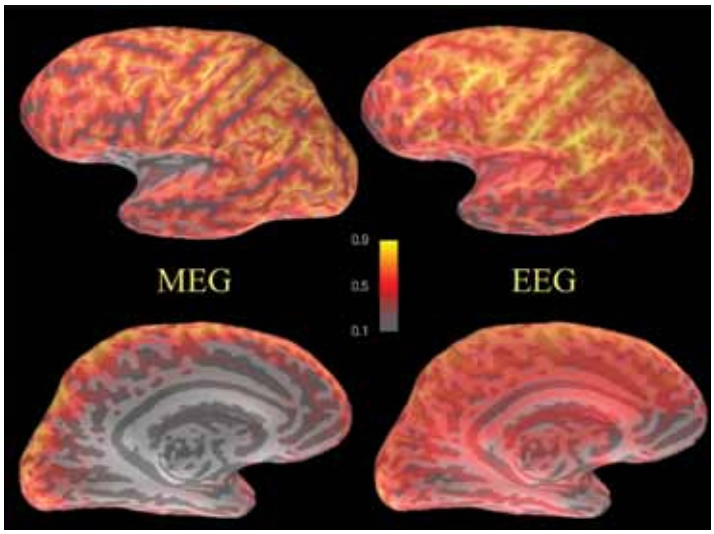

Figure 2. The power of the MEG (left) and EEG (right) signal patterns measured with 102 magnetometers (left) and 60 EEG electrodes (right) generated by current sources normal to the cortex. The maximal value of each distribution is normalized to unity, i.e., the scale bars show fractions of the maximum value. Notice the strong contribution that sources at the crests of the gyri make to EEG and the steep falloff of the MEG signal with depth.

computed using a three-compartment BEM rather than the sphere model. MEG indeed appears almost blind to sources at the crests of the gyri and those at the bottom of the sulci, whereas EEG receives a very strong contribution from the radially oriented gyral sources. This discrepancy means that the signal-to-noise ratio (SNR) of EEG for activity in the sulci is likely to be lower than that of MEG. In a study by Goldenholz et al. (2009), theoretical calculations were further supported by evidence from observations of variable SNRs of epileptic spikes as a function of their location of origin. Figure 2 also clearly shows that deep sources are more weakly reflected in MEG than in EEG. However, as discussed in Attal and Schwartz (2013) and supported by the evidence of MEG being able to detect signals from the deeper structures discussed earlier, the SNR of MEG and that of EEG may be more similar than generally thought.

Because the cortex is heavily folded, MEG and EEG signals originating from the synchronous activation of a large region of cortex probably suffer from cancellation effects due to different source orientations being present. These spatial cancellation effects were recently studied in detail (Ahlfors et al., 2010). The results indicate that both MEG and EEG signals are strongly attenuated because of cortical folding. Also, this attenuation is more significant in MEG than in EEG, when a large ensemble of patches at different locations of the cortex is considered. The reason for the latter difference is most likely the contribution that radial sources make to EEG. In particular, if the activated patch includes a crest of a gyrus and walls of fissures symmetrically on both sides of it, the MEG signals arising from the fissural cortex are canceled out, while the EEG signals arising from the radially oriented currents remain. This phenomenon is illustrated in Figure 3, which simulates the signals arising from the activation of a large patch in the parietal cortex, covering both walls of fissures. The EEG signals indicate the presence of radial currents at the activated site, whereas MEG detects only minor tangential sources in the "outskirts" of the activated patch.

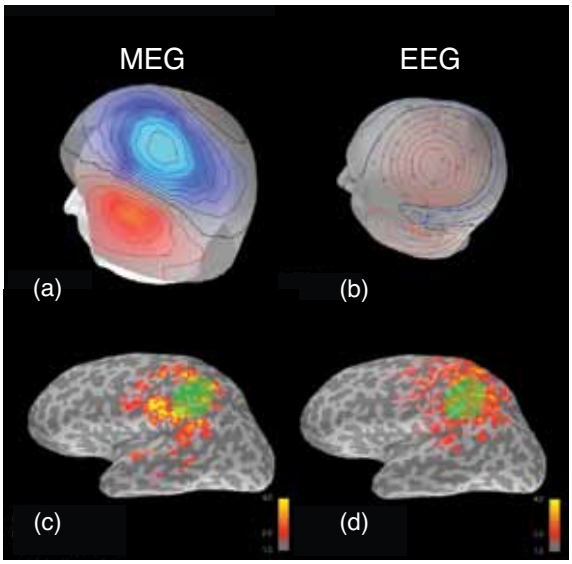

Figure 3. MEG (*a*) and EEG (*b*) signal distributions arising from the activation of a patch of parietal cortex. In ***a,*** the red and blue contours indicate magnetic emerging and entering the head, respectively, while in ***b,*** red and blue indicate the positive and negative potential values. The corresponding minimum-norm current estimates were computed with a cortical constraint and are visualized in an inflated view of the cortex in ***c*** and ***d***. The activated area is shown with green shading. EEG shows activity in cortex with radially oriented currents (light gray areas), whereas the MEG-visible currents in the fissures are largely invisible owing to cancellation between the opposite walls of the sulci.

The Equivalent-Current Dipole Models

The goal of the electromagnetic inverse problem is to estimate the source-current density underlying the MEG or EEG signals measured outside the head. Unfortunately, the primary current distribution cannot be recovered uniquely, even if the magnetic field and/or the electric potential were precisely known everywhere outside the head (Helmholtz, 1853). However, it is often possible to use additional anatomical and physiological information to constrain the problem and to facilitate its solution. One approach is to replace the actual current sources by equivalent generators that are characterized by a few parameters. A unique solution for the parameters may then be obtained from the measured data by a least squares fit. Figure 4 illustrates the concept of the equivalent-current dipole (ECD) source. In this simulation, an extended patch of cortex near the left auditory cortex was activated, and the ECD was fitted to the simulated data. The location of the dipole matches the site of activation well, even though the information of the actual extent is naturally lost.

In the time-varying dipole model, first introduced to the analysis of EEG data (Scherg and von Cramon, 1985; Scherg, 1990), an epoch of data is modeled with a set of current dipoles whose orientations and locations are fixed but whose amplitudes are allowed to vary with time. This approach corresponds to the idea of small patches of the cerebral cortex or other structures being activated simultaneously or in a sequence. As noted, the precise details of the current distribution within each patch cannot be revealed by the measurements, which are performed at a distance in excess of 3 cm from the sources.

NOTES

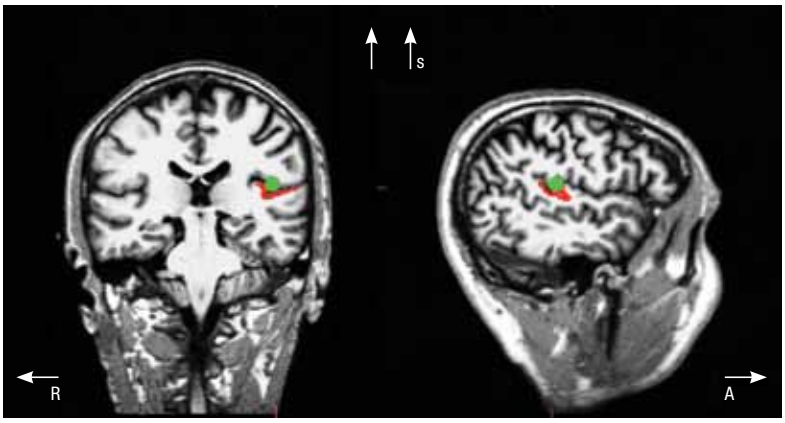

Figure 4. An equivalent-current dipole (green dot) corresponding to an activated patch of cortex (red shading). A, anterior; R, right; S, superior.

Distributed Source Models

An alternative approach to source modeling is to assume that the sources are distributed within a volume or surface (often called the source space) and then to use various estimation techniques to find out the most plausible source distribution. The source space may be either a volume defined by the brain or restricted to the cerebral cortex, determined from MR images (Dale et al., 1999). These techniques can provide reasonable estimates of complex source configurations without having to resort to complicated dipole-fitting strategies.

Inverse solutions that result in a source distribution are commonly referred to as "imaging methods." This nomenclature is motivated by the fact that the current estimate explains the data and can be visualized as an image or a sequence of images. If the sources are limited to the cortex, their orientations can be aligned with the estimated cortical surface normals (Dale and Sereno, 1993). In this case, only the dipole amplitudes need to be estimated. Alternatively, the orientations can be considered unknown, in which case both amplitudes and orientations need to be estimated at each spatial location.

One of the challenges for distributed inverse methods is that the number of dipoles by far exceeds the number of MEG/EEG sensors. Therefore, a priori constraints based on the likely characteristics of the actual source distributions are necessary. Common priors are based on the Frobenius norm and lead to a family of methods generally referred to as minimum-norm estimates (MNEs) (Hämäläinen and Ilmoniemi, 1984). MNEs can be converted into statistical parameter maps, which take into account the noise level, leading to noise-normalized methods such as dSPM (dynamic statistical parametric mapping) (Dale et al., 2000) or sLORETA (standardized low-resolution electromagnetic tomography) (Pascual-Marqui, 2002).

Although these methods have clear benefits, including simple implementation and robustness to noise, they do not take into account the natural assumption that only a few brain regions are typically active during a task. Interestingly, this latter assumption is exactly what justifies the use of discrete dipole-fitting methods. In order to promote such focal or sparse solutions within the distributed source model framework, one uses sparsity-inducing priors (Matsuura and Okabe, 1995; Uutela et al., 1999). However, if such priors are applied time point by time point (using minimum-current estimates, or MCEs), it becomes challenging to obtain consistent estimates of the source orientations as well as temporally meaningful source waveforms.

In order to promote spatiotemporally coherent focal estimates, several publications have proposed constraining the active sources to remain the same over the time interval of interest (Friston et al., 2008; Ou et al., 2009; Wipf and Nagarajan, 2009; Gramfort et al., 2012). The implicit assumption then becomes that the sources are stationary. This conjecture is reasonable for short time intervals. However, it is not a good model for realistic source configurations where multiple transient sources activate sequentially or simultaneously during the analysis period before returning to baseline at different time instants.

We recently addressed the problem of localizing nonstationary focal sources from MEG/EEG data using appropriate sparsity-inducing norms (Gramfort et al., 2013). Extending the work from Gramfort et al. (2012) in which we coined the term "mixed-norm estimates" (MxNEs), we proposed in Gramfort et al. (2013) to use mixed norms defined in terms of the time-frequency decompositions of the sources. We called this approach the time-frequency mixed-norms estimates (TF-MxNE). The benefit of this modification is that the estimates of nonstationary sources can be obtained over longer time intervals while making optional standard preprocessing (e.g., filtering or time-frequency analysis of the sensor signals).

Figure 5 summarizes the spatiotemporal characteristics of different distributed source estimates. The

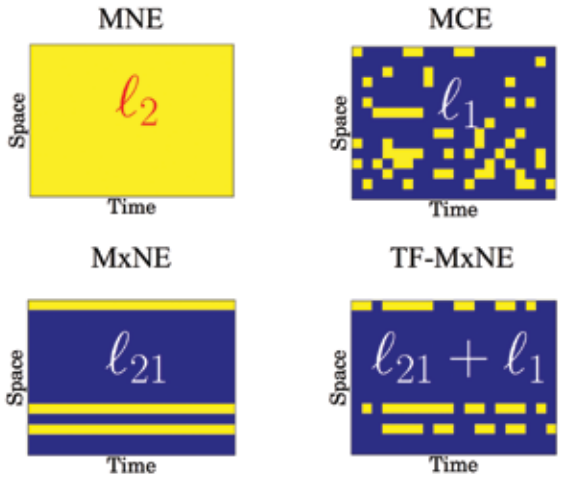

Figure 5. Characteristics of distributed source estimates. MNE, minimum-norm estimate; MCE, minimum current estimate; MxNE, mixed-norm estimate promoting spatial sparsity and temporal smoothness; TF-MxNE, time-frequency mixed-norm estimate allowing for nonstationary time courses.

MNE solutions and statistical maps derived therefrom exhibit nonzero activity at all time points and spatial locations. Therefore, the extents of the activity depend on the statistical thresholding applied. The MCE solution is a sparse estimate computed separately at each time point and, therefore, spatial consistency across time is not warranted. The MxNE solution posited by Ou et al. (2009) and Gramfort et al. (2012) shows consistent locations of activity, but the source amplitudes are nonzero at all time points. Finally, the TF-MxNE solution is sparse in space and locally smooth in time/frequency but allows for nonstationarity of the sources on the global time scale.

Conclusions

Since the relationship of MEG or EEG signals and their sources is fully governed by the Maxwell's equations, the signal distributions arising from given cerebral sources can be simulated accurately. These simulations give several insights into the characteristics of MEG and EEG. For example, MEG is less sensitive to the actual electrical conductivities within the head, and EEG and can thus provide more accurate estimates of the source strengths than can MEG. Furthermore, although MEG receives weaker contributions from deep sources within the brain than EEG, the SNRs of MEG and EEG may actually be similar. The similarity derives from the strong EEG signals arising from very superficial cortical activity; these signals, in turn, are filtered out from MEG owing to the radial orientation of the corresponding sources.

The ambiguity of the inverse problem has been often cited as a major drawback of both EEG and MEG. Both methods thus have had to rely on a restrictive source model, making the analysis rather difficult for a beginner. It is also perhaps confusing to find that several competing source models are available, and sometimes, the authors introducing them are not clear enough about stating the underlying assumptions and their consequences for data interpretation. Fortunately, constraints for the inverse problem can be obtained from other imaging modalities, in particular, anatomical MRI.

We expect in the future major developments in efficient and automated MEG/EEG analysis methods, novel experimental paradigms to fully utilize the benefits of MEG/EEG, and reliable routines to combine MEG/EEG with other imaging modalities. We anticipate that such approaches will significantly increase our understanding of human brain functions, especially their temporal dynamics and the interactions between cortical regions and deeper structures involved in perception, cognition, and action.

References

Ahlfors SP, Han J, Lin FH, Witzel T, Belliveau JW, Hamalainen MS, Halgren E (2010) Cancellation of EEG and MEG signals generated by extended and distributed sources. Hum Brain Mapp 31:140–149.

Attal Y, Schwartz D (2013) Assessment of subcortical source localization using deep brain activity imaging model with minimum norm operators: a MEG study. PloS One 8:e59856.

Dale AM, Sereno MI (1993) Improved localization of cortical activity by combining EEG and MEG with MRI cortical surface reconstruction: a linear approach. J Cogn Neurosci 5:162–176.

Dale AM, Fischl B, Sereno MI (1999) Cortical surface-based analysis. I. Segmentation and surface reconstruction. Neuroimage 9:179–194.

Dale AM, Liu AK, Fischl BR, Buckner RL, Belliveau JW, Lewine JD, Halgren E (2000) Dynamic statistical parametric mapping: combining fMRI and MEG for high-resolution imaging of cortical activity. Neuron 26:55–67.

Friston K, Harrison L, Daunizeau J, Kiebel S, Phillips C, Trujillo-Barreto N, Henson R, Flandin G, Mattout J (2008) Multiple sparse priors for the M/EEG inverse problem. Neuroimage 39:1104–1120.

NOTES

Goldenholz DM, Ahlfors SP, Hamalainen MS, Sharon D, Ishitobi M, Vaina LM, Stufflebeam SM (2009) Mapping the signal-to-noise-ratios of cortical sources in magnetoencephalography and electroencephalography. Hum Brain Mapp 30:1077–1086.

Gramfort A, Kowalski M, Hamalainen M (2012) Mixed-norm estimates for the M/EEG inverse problem using accelerated gradient methods. Phys Med Biol 57:1937–1961.

Gramfort A, Strohmeier D, Haueisen J, Hamalainen MS, Kowalski M (2013) Time-frequency mixed-norm estimates: sparse M/EEG imaging with non-stationary source activations. Neuroimage 70:410–422.

Hämäläinen M, Ilmoniemi R (1984) Interpreting magnetic fields of the brain: minimum norm estimates. Med Biol Eng Comput 32(1):35–42.

Hämäläinen MS, Sarvas J (1989) Realistic conductivity geometry model of the human head for interpretation of neuromagnetic data. IEEE Trans Biomed Eng 36(2):165–171.

Helmholtz H (1853) Ueber einige Gesetze der Vertheilung elektrischer Strome in korperlichen Leitern, mit Anwendung auf die thierisch-elektrischen Versuche. Ann Phys Chem 89:211–233, 353–377.

Hung Y, Smith ML, Bayle DJ, Mills T, Cheyne D, Taylor MJ (2010) Unattended emotional faces elicit early lateralized amygdala-frontal and fusiform activations. Neuroimage 50:727–733.

Matsuura K, Okabe Y (1995) Selective minimum-norm solution of the biomagnetic inverse problem. IEEE Trans Biomed Eng 42:608–615.

Mosher JC, Leahy RM, Lewis PS (1999) EEG and MEG: forward solutions for inverse methods. IEEE Trans Biomed Eng 46:245–259.

Murakami S, Zhang T, Hirose A, Okada YC (2002) Physiological origins of evoked magnetic fields and extracellular field potentials produced by guinea-pig CA3 hippocampal slices. J Physiol 544:237–251.

Okada YC, Wu J, Kyuhou S (1997) Genesis of MEG signals in a mammalian CNS structure. Electroencephalogr Clin Neurophysiol 103:474–485.

Ou W, Hamalainen MS, Golland P (2009) A distributed spatio-temporal EEG/MEG inverse solver. Neuroimage 44:932–946.

Parkkonen L, Fujiki N, Makela JP (2009) Sources of auditory brainstem responses revisited: contribution by magnetoencephalography. Hum Brain Mapp 30:1772–1782.

Pascual-Marqui RD (2002) Standardized low-resolution brain electromagnetic tomography (sLORETA): technical details. Methods Find Exp Clin Pharmacol 24(Suppl D):5–12.

Sarvas J (1987) Basic mathematical and electromagnetic concepts of the biomagnetic inverse problem. Phys Med Biol 32:11–22.

Scherg M (1990) Fundamentals of dipole source potential analysis. In: Auditory evoked magnetic fields and potentials (Grandori F, Hoke M, Romani GL, eds), pp 40–69. Basel: Karger.

Scherg M, von Cramon D (1985) Two bilateral sources of the late AEP as identified by a spatio-temporal dipole model. Electroencephalogr Clin Neurophysiol 62:232–244.

Uutela K, Hämäläinen M, Somersalo E (1999) Visualization of magnetoencephalographic data using minimum current estimates. Neuroimage 10:173–180.

Wipf D, Nagarajan S (2009) A unified Bayesian framework for MEG/EEG source imaging. Neuroimage 44:947–966.

Wolters CH, Grasedyck L, Hackbusch W (2004) Efficient computation of lead field bases and influence matrix for the FEM-based EEG and MEG inverse problem. Inverse Problems 20:1099–1116.